Original Research Article: full paper

(2023), «EUREKA: Physics and Engineering»
Number 3

# A COMPARISON STUDY OF THE BEHAVIORS OF SINGLE-PHASE TURBULENT FLOW AT LOW TO MODERATE REYNOLDS NUMBERS THROUGH A VERTICAL PIPE: 3D COUNTERS ANALYSIS

***Amjed Ahmed Ali***
*Department of Fuel and Energy Engineering*[1]

***Akeel M. Ali Morad***✉
*Department of Fuel and Energy Engineering*[1]
*akeel@stu.edu.iq*

***Rafi M. Qasim***
*Department of Fuel and Energy Engineering*[1]

[1]*Basra Technical Engineering College*
*Southern Technical University*
*Al Zubair Highway str., In front of Basra Sports City, Basra, Iraq, 61003*

✉**Corresponding author**

**Abstract**

The study presented three-dimensional (3D) analysis of water's upward flowing through the vertical pipe under turbulent characteristic considerations. Both numerical constructed and improved the model of 3D for cylindrical coordinates of governing equations for incompressible turbulent flow with the Reynolds Average Navier-Stokes (RANS) model using the improved constants of the ($k$–ε) type. The present model is then compared with a previous study to give the feasibility of the present single-phase turbulent flow parameters. The pipe length is tested to measure how much it affected the turbulent parameters though one of the expected factors is the turbulent time scale. On the other hand, the model is numerically examined to determine the velocity profile, shear rate, and surface deformation of the water domain. While the pressure distribution, turbulent kinetic energy, and turbulent dissipation rate, these parameters are classified as the mechanic's system factors. The simulation is done with wide software used to simulate industrial is COMSOL 5.4 Multiphysics software. The results obtained increased the velocity of three inlet water velocities used ranging from (0.087, 0.105, and 0.123 m/sec) of upward flow. High fluctuation in the water flow moves along the entire pipe length and it can notice the sensitivity to any change in water properties or mechanical properties. The liquid upward flow in turbulent conditions is suffered from many characteristics such them related to liquid properties and others related to the mechanics of the application through the systems. The interaction between the fluid film (fluid boarded the pipe inner diameter) has been observed by the shear rate and liquid surface deformation.

**Keywords:** low Reynolds Number, single-phase vertical flow, turbulent flow, 3D analysis.

**DOI: 10.21303/2461-4262.2023.002854**

## 1. Introduction

The topic of simulation is widely used for both foci and deeply shows the precise change in the system. Cartesian, cylindrical, and spherical coordinates are considered in many types of research for approaching the experimental with numerical models. The three-dimensional analysis of compressible and incompressible fluid flowing into any mechanical engineering implementation is concerning most topics undertaken by limited researchers. There are many applications of the incompressible upward flow through the vertical pipes such as water flowing in the riser and down-comer in the steam generators of the power plant, air-conditioning, and ventilation systems when using cold water coils, fluids pumped in the wells, etc. Therefore, the present work is the development of the mathematical model for single-phase turbulent upward flow.

The paper [1] focused to study the 2D counter analysis of a single turbulent flow. They intended to present the interaction fluid structure near the inside pipe diameter. While the paper [2] is presented the 3D analysis of the pressure drop of fluid flow through fittings. The behavior of fluid motion inside the vertical drilling pipe is presented in [3]. The study [4] is focused on analyzing

the fluid flow inside the pipe with 2D and 3D models in many applications such as pipe networks, Tee-junction, elbow, bending straight pipes at different positions, drilling pipes, etc. These studies used 2D and 3D analysis with helping to solve the model of laminar and turbulent at a single flow. The fluid layer studied by [5] using the turbulent flow conditions in closed conduct is limited by the ($k$–ε) type which depended on the many parameters related to constant and other hands related to model characteristic properties. Many published papers related to developing turbulent flow models through these constants and parameters. Last early twenty years and more effective articles to modify different models like [6]. They remark in conclusion that when using the modified model, it did not need a complex governing equation. The paper [7] is dedicated to the 3D turbulent models consisting of wall functions with CFD-solved by the Reynolds-Averaged Navier-Stokes equations (RANS) method. The study presented the experimental and numerical by [8], they intended to investigate the turbulent flow behavior of ($k$–ε). The model suggested solving the turbulent wall function with numerical analysis for the flat plate boundary layer. The eddy viscosity for the nonlinear Reynolds stress model is numerically studied by [9]. The turbulent flow simulation in cylindrical is considered by [10] a stagnating challenge in the industry, of costs and the tool used to do the simulation. This challenge becomes huge in calculation with the unsteady turbulent flow. They obtained a good agreement on the velocity profile of the steady-state wall shear stress.

The pressure gradient of single-phase turbulent flow described that the laminar flow of the pressure drop is less when the flow is turbulent. The experimental measure was studied by [11, 12] in these studied the turbulent flow for both single and two-phase flow with different tube geometry. There are studies for an inner pipe diameter of (0.026 m) with an airflow rate of (0.02 $m^3$/s). The Reynolds-Averaged Navier-Stokes equations (RANS) model with ($k$–ε) type with large eddy simulation to numerically with solving the models with large eddy simulation which found the high-pressure oscillation $n$ two-phase flow than in single-phase flow greater by 100 times for the RANS model. The Partially Averaged Navier-Stokes (PANS) for the near-wall turbulent associated with Low Reynolds Number (LRN) at fluid flow is displayed by [13]. Two Reynolds numbers were used ranging from (10600 and 37000) for closed channel flow. The effects expression that the PANS model diverged from the RANS model for a channel turbulent flow. Recently, they [14, 15] presented the numerical simulation of fluid flows through the elbow and Tee-junction at turbulent flow depending on the Reynolds number. They approached the simulation model with experimental data to obtain the visualization of the fluid flow through the fittings.

In our study, most of the affected parameters were studied to show the 3D behavior of the water upward at turbulent flow through a vertical pipe. From the above pieces of literature, it concluded to use the RANS model with the ($k$–ε) type. This study is extended to the previous study with a comparison to improve the 3D model. It can notice that the liquid upward flow in turbulent conditions is suffered from many characteristics such them related to liquid properties and others related to the mechanics of the application through the systems. The interaction of liquid motion inside the vertical pipe has many factors raised and different when the 2D and a 3D analysis.

The study aims to present a 3D model of the upward single-phase turbulent flow of incompressible fluid. To achieve this aim, the following objectives are accomplished:

− to describe the numerical model and the validity of the model with previous work with the help of COMSOL 5.4 Multiphysics software;

− to examine the pipe length at different water velocities to observe the effective pipe geometry;

− to study the behavior of the flow parameters at different inlet water velocities;

− to observe turbulent time scale and study the effectiveness of pipe length. Shear rate and surface deformation of the water element are present due to the 2D contours;

− to plot for both turbulent kinetic energy and turbulent dissipated rate.

## 2. Materials and methods

### 2. 1. System of the Navier-Stokes equations

The describing incompressible liquid flow is the system of the Navier-Stokes equations and the continuity equation with three velocities' components in cylindrical coordinates ($\theta$, $r$, $z$) with velocity components of ($u$, $v$, and $w$) [16]:

Equation of continuity:

$$\frac{1}{r}\frac{\partial(rv)}{\partial r}+\frac{1}{r}\frac{\partial(u)}{\partial\theta}+\frac{\partial w}{\partial z}=0. \tag{1}$$

Quantity of movement-radial direction ($r$),

$$\rho\left(v\frac{\partial v}{\partial r}+\frac{u}{r}\frac{\partial v}{\partial\theta}-\frac{u^2}{r}+w\frac{\partial v}{\partial z}\right)=-\frac{\partial p}{\partial r}+\mu\left\{\frac{\partial}{\partial r}\left[\frac{1}{r}\frac{\partial}{\partial r}(rv)\right]+\frac{1}{r^2}\frac{\partial^2 v}{\partial\theta^2}-\frac{2}{r^2}\frac{\partial u}{\partial\theta}+\frac{\partial^2 v}{\partial w^2}\right\}, \tag{2}$$

quantity of movement-tangential or circumferential direction ($\theta$):

$$\rho\left(u\frac{\partial u}{\partial r}+\frac{u}{r}\frac{\partial u}{\partial\theta}+\frac{vu}{r}+w\frac{\partial v}{\partial z}\right)=-\frac{1}{r}\frac{\partial p}{\partial\theta}+\mu\left\{\frac{\partial}{\partial r}\left[\frac{1}{r}\frac{\partial}{\partial r}(ru)\right]+\frac{1}{r^2}\frac{\partial^2 u}{\partial\theta^2}+\frac{2}{r^2}\frac{\partial v}{\partial\theta}+\frac{\partial^2 u}{\partial w^2}\right\}, \tag{3}$$

quantity of movement $z$-axial direction:

$$\rho\left(v\frac{\partial w}{\partial r}+\frac{u}{r}\frac{\partial w}{\partial\theta}+w\frac{\partial w}{\partial z}\right)=\rho g-\frac{\partial p}{\partial z}+\mu\left\{\frac{1}{r}\frac{\partial}{\partial r}\left(r\frac{\partial w}{\partial r}\right)+\frac{1}{r^2}\frac{\partial^2 w}{\partial\theta^2}+\frac{\partial^2 w}{\partial z^2}\right\}, \tag{4}$$

where $\rho$ and $\mu$ are fluid density and fluid dynamic viscosity, respectively.

The turbulent flow modeling equations of tensors have been explained in great detail by [17]:

$$\left\{\rho\frac{\partial\tau_{ij}}{\partial t}\right\}+\left\{\rho u_k\frac{\partial\tau_{ij}}{\partial x_j}\right\}=\left\{-\rho\left(\tau_{ik}\frac{du_j}{\partial x_k}+\tau_{jk}\frac{du_i}{\partial x_k}\right)\right\}+\left\{\frac{\partial}{\partial x_k}\left(\frac{\mu_t}{\sigma_k}\frac{\partial\tau_{ij}}{\partial x_k}\right)\right\}+$$
$$+\left\{\frac{\partial}{\partial x_k}\left(\mu\frac{\partial\tau_{ij}}{\partial x_k}\right)\right\}+\left\{-\frac{2}{3}\in\delta_{ij}\right\}+\{\varphi_{ij}\}, \tag{5}$$

and

$$\left\{\rho\frac{\partial\varepsilon}{\partial t}\right\}+\left\{\rho u_j\frac{\partial\varepsilon}{\partial x_j}\right\}=\left\{\rho C_{\varepsilon 1}\frac{\varepsilon}{k}\tau_{ij}\frac{\partial u_i}{\partial x_j}\right\}+\left\{\frac{\partial}{\partial x_j}\left(\frac{\mu_t}{\sigma_E}\frac{\partial\varepsilon}{\partial x_j}\right)\right\}+\left\{\frac{\partial}{\partial x_j}\left(\mu\frac{\partial\varepsilon}{\partial x_j}\right)\right\}+\left\{-C_{\varepsilon 2}\frac{\varepsilon^2}{k}\right\}. \tag{6}$$

Here, the eddy viscosity term ($\mu_t$) is modeled using the Bossiness approximation (6) as done in the case of the ($k$–$\varepsilon$) equation:

$$\mu_t=C_\mu\rho\frac{k^2}{\varepsilon}. \tag{7}$$

In (6) are set values that are, $\sigma_k=0.82$, $\sigma_\varepsilon=1.0$, $C_\mu=0.09$, $C_{\varepsilon 1}=1.44$, and $C_{\varepsilon 2}=1.92$.

**2. 2. Physical model**

In this paper, the simulation of 3D upward water flows through the vertical pipe at turbulence flow is presented. COMSOL Multiphysics 5.4 was used to generate the domain to show the inlet, outlet, and water boundaries at flow as shown in **Fig. 1**. The pipe domain was created using a (50.8 mm) diameter and a pipe length of (1000 mm). Three inlet water velocities were used ranging from (0.087, 0.105, and 0.123 m/sec).

The verification of pipe length effects was achieved by three length ranges (1000, 1200, and 1400 mm). Moreover, the operation parameters were reported in the provirus study [1].

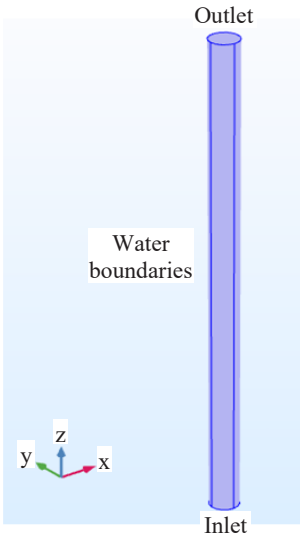


**Fig. 1.** Water domain geometry

**2. 3. Turbulent flow model (*k*–ε)**

There are two kinds of turbulent models in COMSOL Multiphysics software 5.4 (*k*–ε) for 3D modeling, they can summarize as Reynolds Average Navier-Stokes (RANS) and Large Eddy Simulation (LES). The LES is implied with any change in the stream flow, while the RANS is more realized for straight flow. Below is the model of the pipe geometry of the water boundaries domain:

$$k = (\mu + \mu_T)(\nabla u + (\nabla u)^T), \tag{8}$$

and

$$\rho(u \cdot \nabla)k = \nabla \cdot \left[-pI + K\right] + F + \rho g, \tag{9}$$

$$\rho(u \cdot \nabla)k = \nabla \cdot \left[\left(\mu + \frac{\mu_T}{\sigma_k}\right)\nabla k\right] + P_k - \rho\varepsilon, \tag{10}$$

and

$$\rho(u \cdot \nabla)\varepsilon = \nabla \cdot \left[\left(\mu + \frac{\mu_T}{\sigma_\varepsilon}\right)\nabla \in\right] + C_{\varepsilon 1}\frac{\varepsilon}{K}P_k - C_{\varepsilon 2}\rho\frac{\varepsilon^2}{k},\ \varepsilon = ep. \tag{11}$$

The terms $\sigma_k$, $\sigma_\varepsilon$, $C_\mu$, $C_{\varepsilon 1}$, and $C_{\varepsilon 2}$ in the above equation are set to their modified values that are, $\sigma_k = 1$, $\sigma_\varepsilon = 1.3$, $C_\mu = 0.09$, $C_{\varepsilon 1} = 1.44$, and $C_{\varepsilon 2} = 1.92$.

The autocorrection of the turbulence time scale modeled by [18–20] is as follows Turbulence time scale:

$$T_L = \int_0^\infty \rho_L(\tau)\mathrm{d}\tau. \tag{12}$$

**2. 4. Model approaches**

To demonstrate the behavior of 3D upward water flows at turbulence in a vertical pipe with cylindrical coordinates, COMSOL 5.4 Multiphysics software was used to show the behavior when the water warded flows in a vertical pipe. **Fig. 2** shows the part mesh generated which runs the model with optimum convergence of the test. In **Table 1**, the statistical parameters of the meshing accounted for the water domain system. The turbulent flow of the (*k*–ε) model used for testing re-solutions was three deferential water velocities used in the previous study [1].

The 3D analysis of upward water flow in a vertical pipe used the CFD technique for several turbulent Re numbers of (4419, 5339, and 6248).

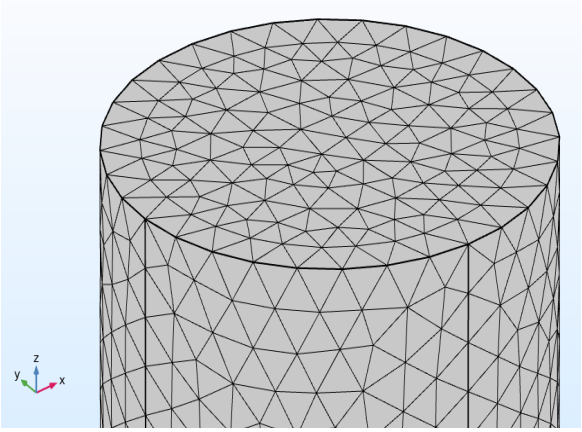


**Fig. 2.** 3D cylindrical generated mesh

**Table 1**
A mesh statistical of water domain geometry

| Description | Value |
|---|---|
| Minimum element quality | 0.2139 |
| Average element quality | 0.6842 |
| Tetrahedron | 286027 |
| Triangle | 16916 |
| Edge element | 884 |
| Vertex element | 8 |
| Maximum element size | 4.88 |
| Minimum element size | 1.46 |
| Curvature factor | 0.6 |
| Resolution of narrow regions | 0.7 |

## 3. Results of numerical model and simulation

### 3. 1. The comparison between the results for modifying the constants of the turbulent flow ($k$–ε) model

**Fig. 3** shows the comparison between the results for modifying the constants of the turbulent flow ($k$–ε) model of the present work with previous work as shown in the values of the constants in **Table 2**. The best observation values into the velocity profile along the pipe diameter. The percentage deviation found at the inlet of the pipe which is also used by [2, 5] at the inlet water velocity is (0.087 m/sec). The minimum to maximum deviation percentage is range from (0.0067 % to 0.0081 %). It can notice from **Fig. 3** that the divergence between the present work results and with previous work is obtained at maximum values of the fluid velocities.

**Table 2**
Comparing the preset work with previous work on the constants of the turbulent flow ($k$–$\varepsilon$) model

| Constants | Present workна | Provirus work [2, 5] |
|---|---|---|
| $C_{\varepsilon 1}$ | 1.44 | 1.45 |
| $C_{\varepsilon 2}$ | 1.92 | 1.9 |
| $C_{\mu}$ | 0.99 | 0.99 |
| $\sigma_k$ | 1.3 | 0.82 |
| $\sigma_{\varepsilon}$ | 1 | 1.3 |

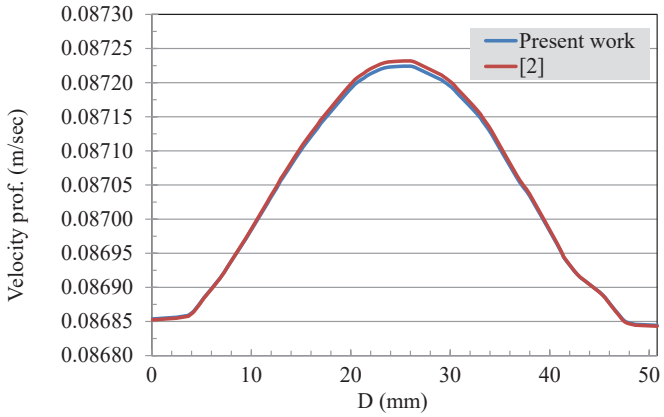


**Fig. 3.** The comparison between the present works with previous works

**Fig. 3** shows an approximate starting velocity deviation before the center of pipe diameter by (17 mm) and by symmetrically after the center of diameter at the distance of (34 mm). It can conclude that the present model is worthily used for the 3D water at turbulent flow upward in a vertical pipe.

The following results show the variation of water upward turbulent flow in a vertical pipe at different pipe lengths ($L$ = 1, 1.2, and 1.4 m) for a pipe diameter of (50.8 mm) and the absolute inlet velocity is (0.0087 m/sec). **Fig. 4** shows the insignificant effect of the pipe length on the turbulent time scale of water flowing through the pipe. It can depend on the pipe length (1 m) for the 3D analysis.

In **Fig. 5**, the turbulent time scale is shown at three different absolute water velocities. The turbulent time scale is represented as the scalar of turbulent flow along the pipe length, and the actions of molecules of fluid (especially the liquids) directly affect and diffuse due to the more shearing force with a solid wall. From **Fig. 4**, it is possible to justify the effects of the difference in pipe lengths. Here, **Fig. 5** shows the variation of the water velocities on the turbulent time scale at the center line along the pipe length.

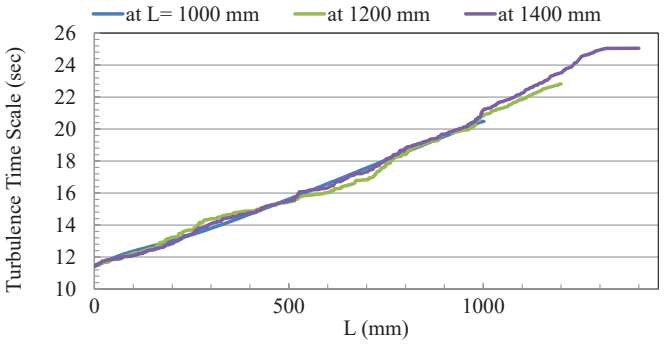


**Fig. 4.** Turbulent time scale with three different pipe lengths

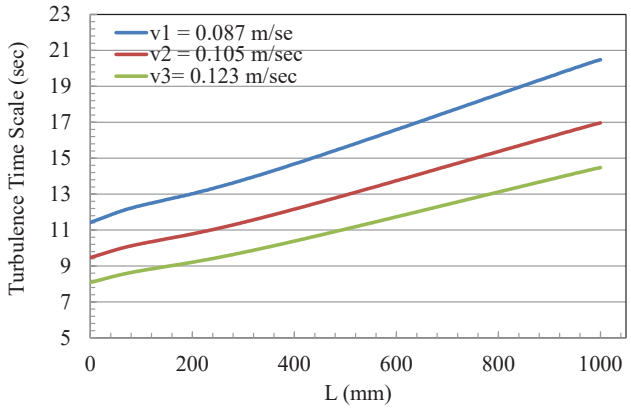


**Fig. 5.** Turbulent time scale at three different water velocities

Here, **Fig. 5** shows the variation of the water velocities on the turbulent time scale at the center line along the pipe length. While **Fig. 6** shows the turbulent time scale contour at ($x$, $z$-plane) perpendicular to the ($y$-plane). Three absolute water velocities were plotted to give the variation of the turbulent time scale when the upward flowing in a vertical pipe.

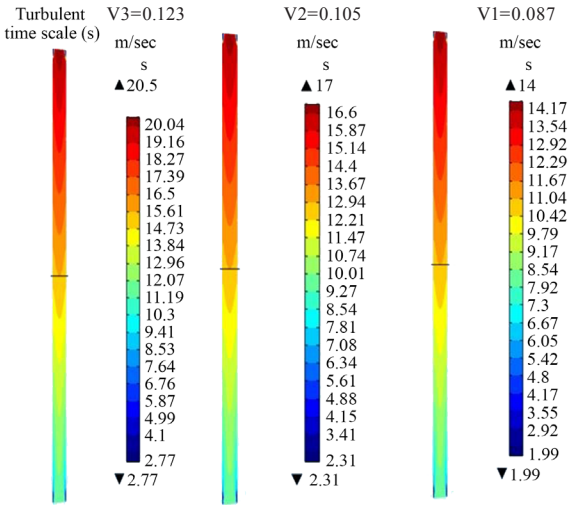


**Fig. 6.** Contour of turbulent time scale at three different water velocities

### 3. 2. Velocity magnitude along the pipe length

To demonstrate the magnitude velocities of the water flow inside the centerline along the length of the pipe. In **Fig. 7** many lines were plotted to show the result with multi-zones along the pipe length. The centerline, (0.4 mm) near the pipe wall, and (2 mm near the pipe wall) were shown in the red lines. **Fig. 8** shows the three velocities at the centerline of the color lines (Blue = 0.087, Green = 0.105, and Red = 0.123 m/sec). At the inlet, the velocity increased slightly, and then the lines are slightly decreased until reach the outlet the velocities become increase in the core of the pipe.

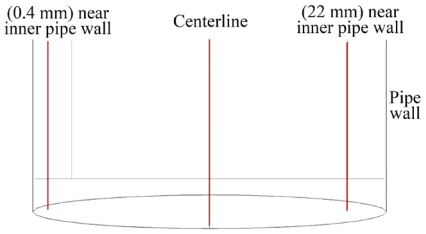


**Fig. 7.** Multi-region line distribution inside along the pipe length

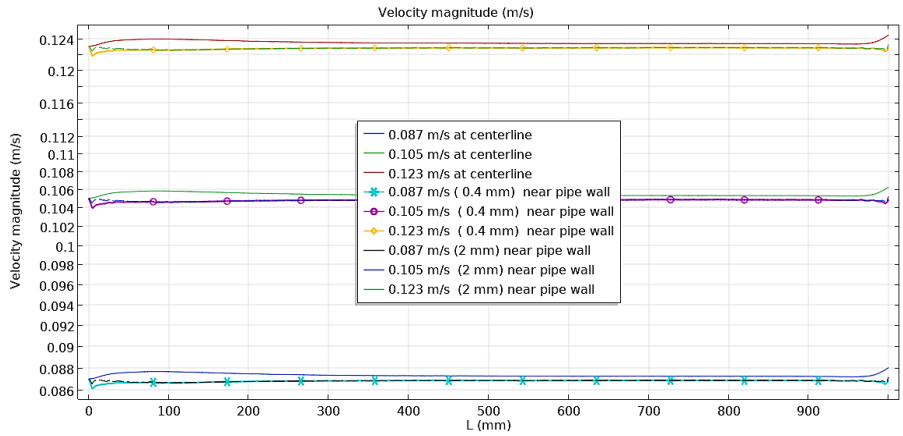


**Fig. 8.** Velocity profile inside along pipe length with three water velocities

The line is far from the inside pipe wall by (0.4 mm), the velocity magnitude being less in value than at the line far (2 mm) from the inner pipe wall. Due to the decrease in the shearing force and the static pressure become less toward the centerline of the inner pipe.

### 3. 3. Shear rate profile and surface deformation of the water element

**Fig. 9** explains the shear rate near the inner pipe wall at the radius of the inlet and the outlet from the pipe. **Fig. 8** shows at any increase in the velocity of water the shear rate increase too at the inner pipe wall, while it decreases at the center of the pipe, that because of the decreases in static pressure. It can be noted from **Fig. 9** that the shear rate at the outlet is greater in value than at the inlet, that because of more accumulative deformation in the fluid layer (water) which is gained when the higher friction of water flows along the pipe. **Fig. 10, 11** show the group contour of the shear rate at the inlet and outlet diameter of the inner pipe respectively.

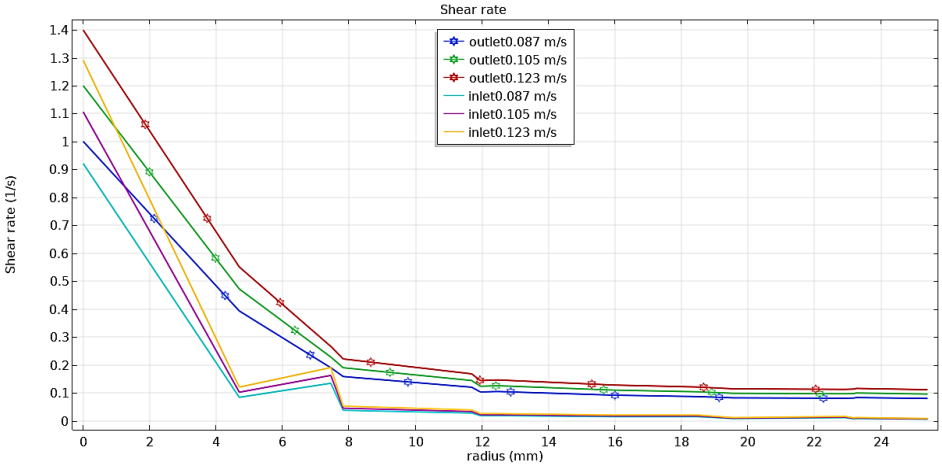


**Fig. 9.** Shear rate vs pipe radius at the inlet and the outlet radius of the pipe

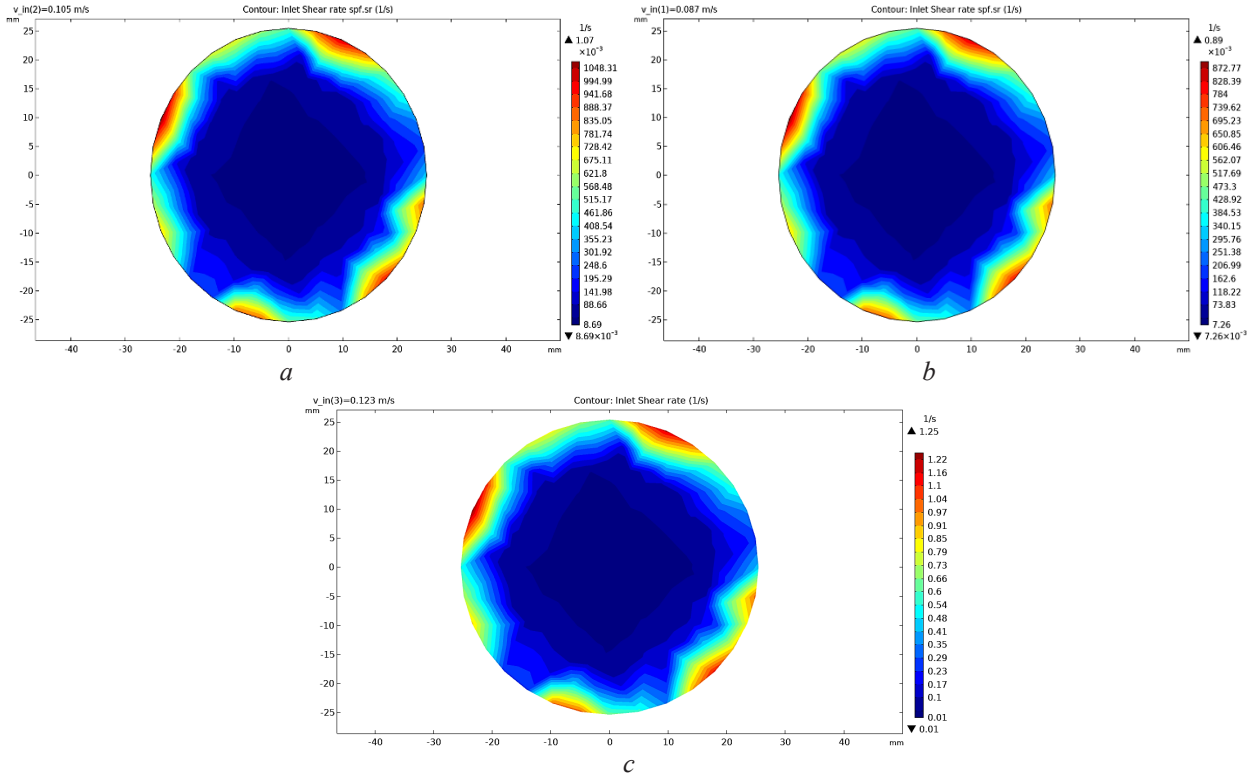


**Fig. 10.** The shear rate at the inlet of three water velocities ($v1$, $v2$, and $v3$)

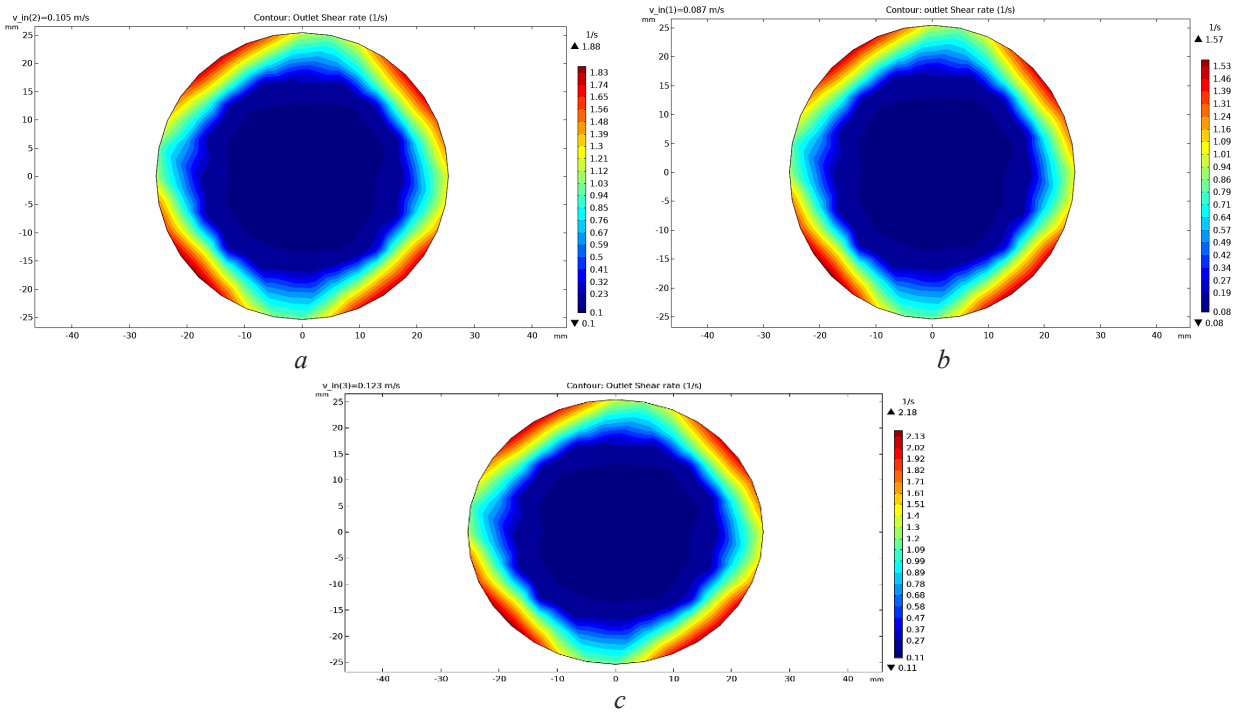


**Fig. 11.** The shear rate at the outlet of three water velocities ($v1$, $v2$, and $v3$)

**Fig. 12** explains the shear rate generated inside along the pipe length. The fluctuation with the variations of the shear rate eddies through the water flowing at three test velocities. The shear rate increases at the inlet of the pipe at a short distance and then decrease until slightly fluctuated along the pipe length in the centerline. At the outlet of the pipe, the shear rate increased due to the directly proportional shear rate with velocities.

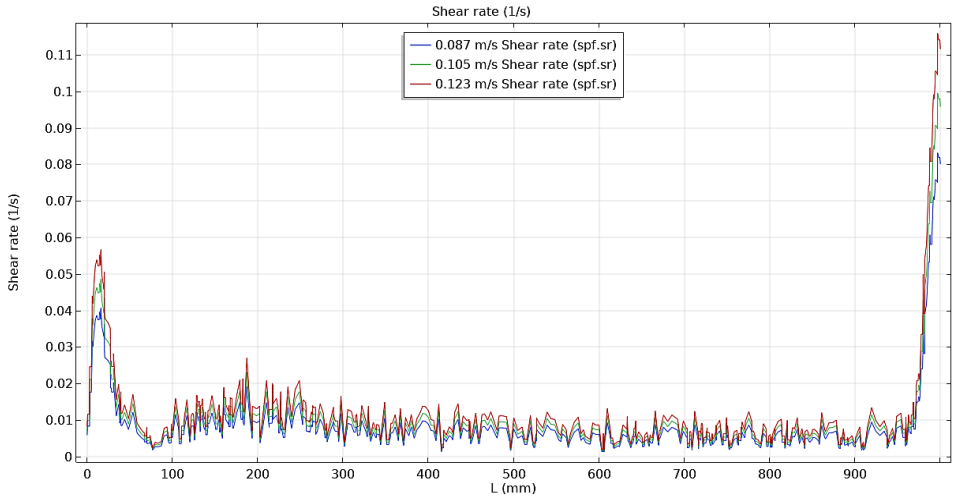


**Fig. 12.** The shear rate along the pipe length of three water velocities ($v1$, $v2$, and $v3$)

**Fig. 13** illustrated the total deformation of the water element flowing inside the pipe. Under a 3D simulation when water is pumped upward in a vertical pipe, this acts as a forced draught system on the water element and led the clutch to deform the water element in an inlet and outlet due to the change in the exerted pressure on it [3].

In **Fig. 12** the borders of three velocities vary to show the water element surface is deformed. At any increase in the water velocity, the surface deformation rate will be increased, that because more pumping pressure with gravity action will occur on the water element.

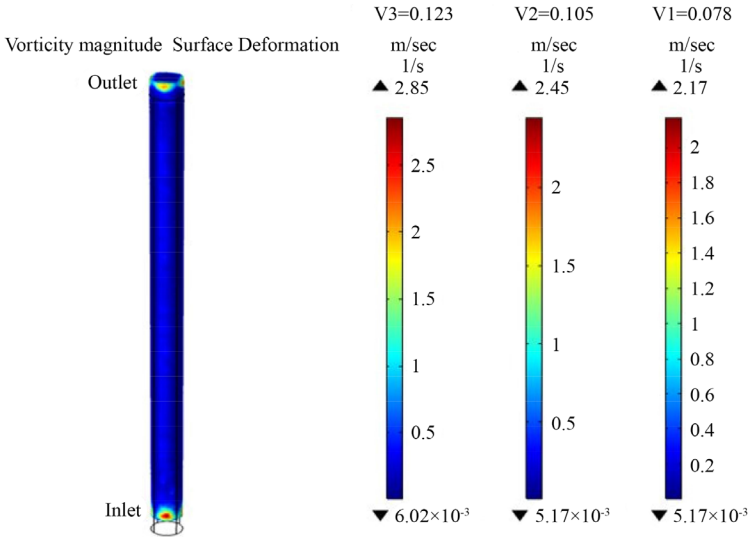


**Fig. 13.** Surface deformation along pipe length of three water velocities ($v1$, $v2$, and $v3$)

### 3. 4. Pressure distribution through the vertical pipe

**Fig. 14** explained the behavior of the pressure distribution of water elements inside the vertical pipe. Due to the water upward flowing inner vertical pipe, many factors affect the flow stream, such as pressure, shear rate, deformation, and the velocity gradient as well as the characteristics factor of turbulent flow, which will explain in the next session. Know **Fig. 14** boarded variations of the water velocities on the pressure profile inside the pipe.

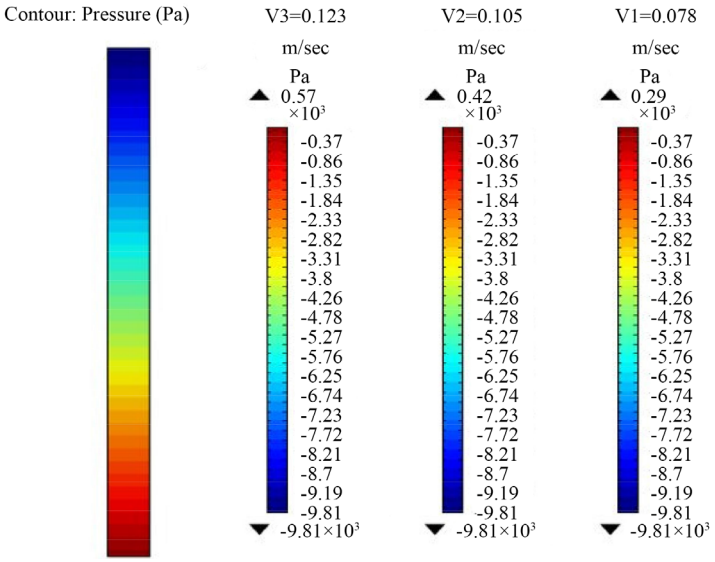


**Fig. 14.** Pressure distribution along pipe length of three water velocities ($v1$, $v2$, and $v3$)

From **Fig. 14** can be obtained that at any increase in the water velocity at the inlet of the vertical pipe, the pressure gradient increases, and then the pressure will decrease until reaches the atmospheric pressure at the outlet of the pipe.

### 3. 5. Turbulent kinetic energy and turbulent dissipation rate

The turbulent kinetic energy of the fluid flowing upwards can be represented with the Isosurface in 3D simulation. **Fig. 15** shows the results of three velocities of the water flowing

upward inside the vertical pipe. These results clearly show the fluctuation motion which is converted by the mean motion velocity.

The Isosurface plotted in **Fig. 15** can also show the thin layer of the boundary and how it deformed due to the flow forcing that pushed the water upwards. A high water velocity leads to giving a high turbulent kinetic energy realized because of the most fluid motion. In the same trend, **Fig. 16** shows the turbulent dissipation rate of water flowing upward in three vertical pipes at three different velocities.

For **Fig. 15, 16** the 3D plotted at the total number of the levels is (14), to show the number of deviations between the turbulent kinetic energy and the dissipation rate of the water element flowing inside the vertical pipe.

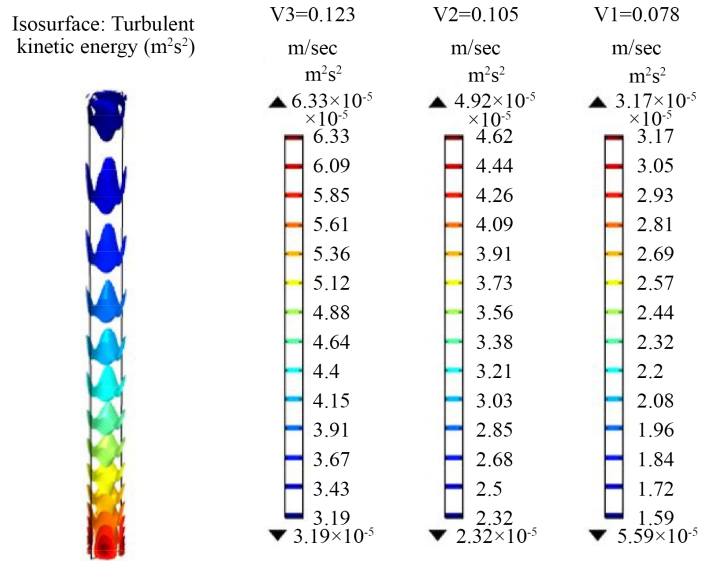


**Fig. 15.** Turbulent kinetic energy along pipe length of three water velocities ($v1$, $v2$, and $v3$)

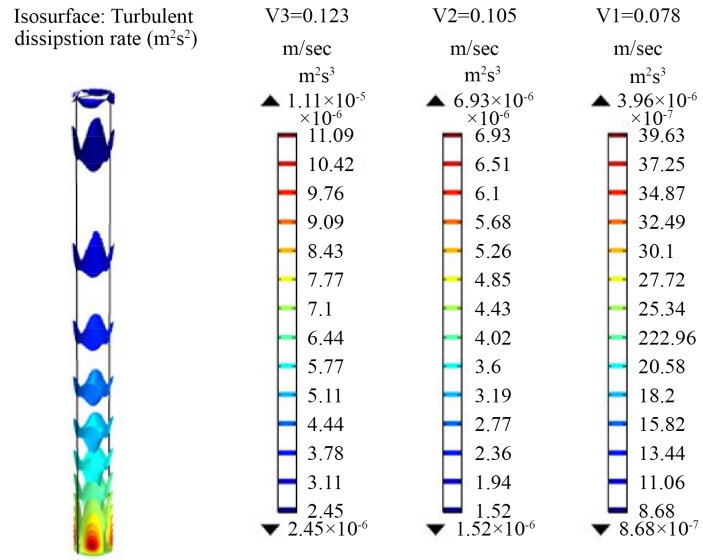


**Fig. 16.** Turbulent dissipation rate along pipe length of three water velocities ($v1$, $v2$, and $v3$)

The dissipation rate changed gradually and dissipated in the direction of flow, that because the momentum despaired from the water boundary layer near the inner pipe wall.

**Fig. 17** summarized both changes in the turbulent kinetic energy and turbulent dissipation rate of the water element. Most of these changes it is difficult to represent especially in 3D analysis, these days, helpful tools are used to observe these changes.

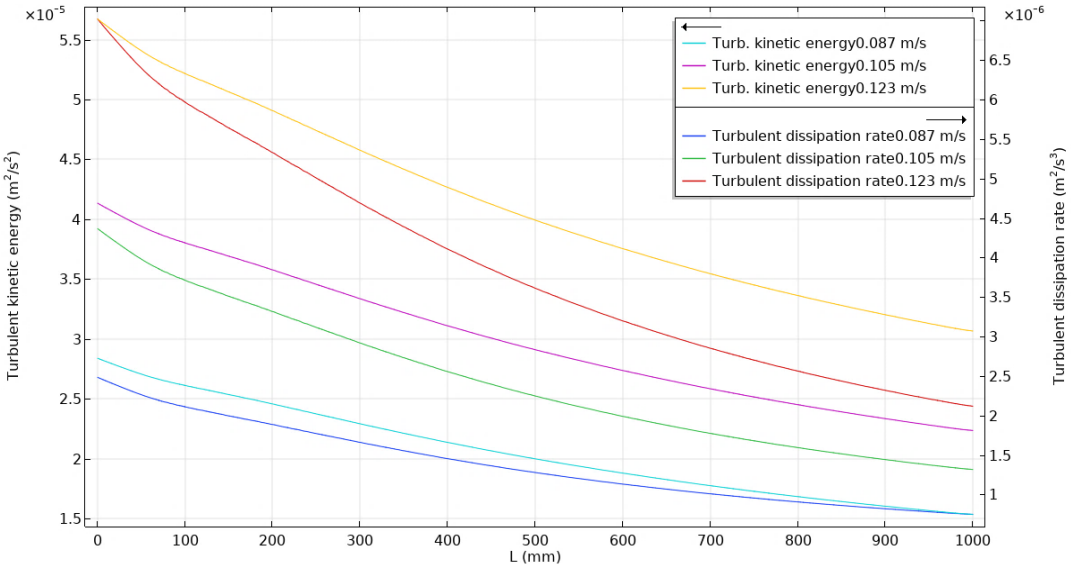


**Fig. 17.** Summarized the changes of the turbulent kinetic energy and turbulent dissipation rate

## 4. Discussion of the numerical model

From the results of **Fig. 4, 5**, it is possible to see the explanation of the insignificant effect of pipe length of more than (1 m) for 3D contour analysis for single-phase turbulent upward flow.

The numerical simulation is solved with the assistance of the COMSOL Multiphysics 5.4 software, which carried out the most effective factors of water flowing upwards inside along the vertical pipe.

The model is developed for a single-phase turbulent upward flow of incompressible fluids.

For the horizontal and inclined pipe, multi-phase flow the model's parameters needed to verify with experimental work.

The numerical analysis is focused on the following behavior such as (variations in water velocities, pressure distribution, shear rate with surface deformation, kinetic energy, and dissipation rate at turbulent flow.

## 5. Conclusions

There is an insignificant pipe-length effect on the behavior of 3D analysis of the turbulent time scale up to (1.1 m).

Three different water-flowing velocities were examined in the turbulent model modified to the ($k$–ε) type and then verified the modified model was with previous work. The pipe was divided into three parts to show the influences of changes in water velocities.

One of the important parameters considered to motivate the action of the fluid motion of the amount of the wall shear rate of the boundary layer near the pipe wall. It is how much the layer of water element surface will be deformed at any change in water velocity with primarily the change of pressure distribution along the pipe length.

The effect of increasing the water flowing over upward velocity in the amount of the turbulent kinetic energy and turbulent dissipation rate has been shown and examined perfectly through the 3D simulation.

Both instantaneously increase the turbulent kinetic energy at any increase in the water velocity and turbulent dissipation rate were designated. Finally, from the comparison with previous work, the modification model of turbulent flow is verified to use with proof of the reliability model.

**Conflict of interest**

The authors declare that they have no conflict of interest in relation to this research, whether financial, personal, authorship, or otherwise, that could affect the research and its results presented in this paper.

**Financing**

The study was performed without financial support.

**Data availability**

The manuscript has data included as electronic supplementary material.

**References**

[1] Morad, A. M. A., Qasim, R. M., Ali, A. A. (2020). Study of the behaviours of single-phase turbulent flow at low to moderate reynolds numbers through a vertical pipe. Part I: 2D counters analysis. EUREKA: Physics and Engineering, 6, 108–122. doi: https://doi.org/10.21303/2461-4262.2020.001538

[2] Moujaes, S. F., Deshmukh, S. (2006). Three-Dimensional CFD Predications and Experimental Comparison of Pressure Drop of Some Common Pipe Fittings in Turbulent Flow. Journal of Energy Engineering, 132 (2), 61–66. doi: https://doi.org/10.1061/(asce)0733-9402(2006)132:2(61)

[3] Ateeq, A. A., Alshamkhani, M. T., Morad, A. M. A. (2020). Conductance Study on The Effect of Torsion of Drilling Pipe on The Inside Pattern Fluid Flow. Journal of Advanced Research in Fluid Mechanics and Thermal Sciences, 75 (2), 185–198. doi: https://doi.org/10.37934/arfmts.75.2.185198

[4] Gajbhiye, B. D., Kulkarni, H. A., Tiwari, S. S., Mathpati, C. S. (2020). Teaching turbulent flow through pipe fittings using computational fluid dynamics approach. Engineering Reports, 2 (1). doi: https://doi.org/10.1002/eng2.12093

[5] Nagano, Y., Tagawa, M. (1990). An Improved $k$–ε Model for Boundary Layer Flows. Journal of Fluids Engineering, 112 (1), 33–39. doi: https://doi.org/10.1115/1.2909365

[6] Argyropoulos, C. D., Markatos, N. C. (2015). Recent advances on the numerical modelling of turbulent flows. Applied Mathematical Modelling, 39 (2), 693–732. doi: https://doi.org/10.1016/j.apm.2014.07.001

[7] Knopp, T. Model-consistent universal wall-functions for RANS turbulence modelling. Available at: https://num.math.uni-goettingen.de/bail/documents/proceedings/knopp.pdf

[8] Zhao, M., Ghidaoui, M. S. (2006). Investigation of turbulence behavior in pipe transient using a $k$–ε model. Journal of Hydraulic Research, 44 (5), 682–692. doi: https://doi.org/10.1080/00221686.2006.9521717

[9] Gatski, T. B., Jongen, T. (2000). Nonlinear eddy viscosity and algebraic stress models for solving complex turbulent flows. Progress in Aerospace Sciences, 36 (8), 655–682. doi: https://doi.org/10.1016/s0376-0421(00)00012-9

[10] Moghaddas, J. S., Trägårdh, C., Östergren, K., Revstedt, J. (2004). A Comparison of the Mixing Characteristics in Single- and Two-Phase Grid-Generated Turbulent Flow Systems. Chemical Engineering & Technology, 27 (6), 662–670. doi: https://doi.org/10.1002/ceat.200401986

[11] Cheng, Y., Lien, F. S., Yee, E., Sinclair, R. (2003). A comparison of large Eddy simulations with a standard $k$–ε Reynolds-averaged Navier-Stokes model for the prediction of a fully developed turbulent flow over a matrix of cubes. Journal of Wind Engineering and Industrial Aerodynamics, 91 (11), 1301–1328. doi: https://doi.org/10.1016/j.jweia.2003.08.001

[12] Morad, A. M. A. (2018). A Two-Phase Pressure Drop Model for Homogenous Separated Flow for Circular Tube Condenser, Examined with Four Modern Refrigerants. Journal of Advanced Research in Fluid Mechanics and Thermal Sciences, 52 (2), 274–287. Available at: https://www.akademiabaru.com/submit/index.php/arfmts/article/view/2401

[13] Kim, J., Yadav, M., Kim, S. (2014). Characteristics of Secondary Flow Induced by 90-Degree Elbow in Turbulent Pipe Flow. Engineering Applications of Computational Fluid Mechanics, 8 (2), 229–239. doi: https://doi.org/10.1080/19942060.2014.11015509

[14] Murthi, A., Reyes, D., Girimaji, S., Basara, B. (2010). Turbulent Transport Modelling for PANS and Other Bridging Closure Approaches. Proceedings of V European Conference on CFD, ECCOMAS CFD. Available at: http://congress2.cimne.com/eccomas/proceedings/cfd2010/papers/01864.pdf

[15] Lee, M. W., Yu, K. H., Teoh, Y. H., Lee, H. W., Ismail, M. A. (2020). Developing Flow of Power-Law Fluids in Circular Tube Having Superhydrophobic Transverse Grooves. Journal of Advanced Research in Fluid Mechanics and Thermal Sciences, 56 (1). Available at: https://www.akademiabaru.com/submit/index.php/arfmts/article/view/2480

[16] Biswas, G, Eswaran, V. (2002). Turbulent Flows, Fundamentals, Experiments and Modeling. IIT Kanpur Series of Advanced Texts. Alpha Science, 456.

[17] Saemi, S., Raisee, M., Cervantes, M. J., Nourbakhsh, A. (2018). Computation of two- and three-dimensional water hammer flows. Journal of Hydraulic Research, 57 (3), 386–404. doi: https://doi.org/10.1080/00221686.2018.1459892

[18] Frost, W., Moulden, T. H. (Eds.) (1977). Handbook of Turbulence. Springer, 498. doi: https://doi.org/10.1007/978-1-4684-2322-8

[19] O'Neill, P. L., Nicolaides, D., Honnery, D., Soria, J. (2004). Autocorrelation Functions and the Determination of Integral Length with Reference to Experimental and Numerical Data. 15th Australasian Fluid Mechanics Conference. Available at: https://www.academia.edu/20918382/Autocorrelation_Functions_and_the_Determination_of_Integral_Length_with_Reference_to_Experimental_and_Numerical_Data

[20] Biletsky, V., Vitryk, V., Mishchuk, Y., Fyk, M., Dzhus, A., Kovalchuk, J. et al. (2018). Examining the current of drilling mud in a power section of the screw downhole motor. Eastern-European Journal of Enterprise Technologies, 2 (5 (92)), 41–47. doi: https://doi.org/10.15587/1729-4061.2018.126230

*Received date 13.12.2022*
*Accepted date 28.02.2023*
*Published date 25.05.2023*



***How to cite:*** *Ali, A. A., Morad, A. M. A., Qasim, R. M. (2023). A comparison study of the behaviors of single-phase turbulent flow at low to moderate Reynolds numbers through a vertical pipe: 3D counters analysis. EUREKA: Physics and Engineering, 3, 15–28. doi: https://doi.org/10.21303/2461-4262.2023.002854*